sPHENIX Report

tag: sPH-CONF-COLDQCD-2025-01
version: 1.0
DOI: unspecified
date: March 18, 2025

Measurement of Transverse Single-Spin Asymmetries in π^0 and η Meson Production in $\sqrt{s} = 200$ GeV $p^{\uparrow} + p$ Collisions with sPHENIX

The sPHENIX Collaboration

Abstract

The sPHENIX experiment is a next-generation collider detector at the Relativistic Heavy Ion Collider (RHIC) designed for rare jet and heavy-flavor probes of Au+Au and polarized p+p collisions. The experiment includes a large acceptance, granular electromagnetic calorimeter and very high-rate data acquisition plus trigger system. In the RHIC Run-2024, sPHENIX collected data from the collisions of transversely polarized protons at $\sqrt{s} = 200$ GeV using calorimeter-based, high-energy jet and photon triggers. This note describes the extraction of transverse single-spin asymmetries in inclusive forward production of π^0- and η-mesons decaying into two photons, the first transverse single-spin asymmetry extracted from sPHENIX data. Such observables are sensitive to multi-parton correlations in the proton, which are related to transverse-momentum dependent (TMD) effects. The results are reported for meson transverse momenta between 3 GeV and 10 GeV (3 GeV and 20 GeV) for the π^0 (η) meson and are compared to PHENIX RHIC Run-2015 data.

1 Introduction

The measurement of large transverse single-spin asymmetries A_N in the forward direction in high-energy hadron-hadron scattering processes [1], which are not adequately explained by the collinear, leading-twist perturbative quantum chromodynamics (QCD) framework, has driven significant development in the field of QCD with transverse-momentum dependent (TMD) degrees of freedom. The A_N is generically defined as a left-right asymmetry in particle production, where "left" and "right" are defined relative to the spin direction of the vertically-polarized hadron beam.

The sizable A_N's are attributed to two prominent TMD effects - the Sivers [2, 3] and Collins [4] effects. The initial-state Sivers effect describes the correlation of parton transverse momentum k_T to the transverse nucleon spin. The final-state Collins effect describes the fragmentation of a transversely polarized quark into an unpolarized hadron and is expressed as the correlation of the spin of the fragmenting parton to the angular distribution of the produced hadrons. Alternatively, the collinear twist-3 (CT3) scheme [5] identifies intrinsic interference between multi-parton states as the generator of the A_N. The CT3 framework distinguishes tri-gluon (ggg) and quark-gluon-quark (qgq) correlation functions referred to as twist-3 multiparton correlators. In analogy to the TMD framework [6], they come as Sivers-(Qiu-Sterman)- or Collins-(fragmentation)-like correlators, which can be shown to be related to k_T-moments of TMD parton distribution functions (PDFs) or fragmentation functions [7], respectively.

In this analysis, the A_N is extracted in inclusive production of π^0- and η-mesons in RHIC Run-2024 proton-proton collisions, $p^\uparrow p \to \pi^0 X$ and $p^\uparrow p \to \eta X$, where one of the proton beams is transversely polarized. This measurement is at moderate forward rapidities $\eta > 0$ with respect to the polarized beam. The neutral mesons are analyzed in their di-photon decay channel and are identified by characteristic signatures in the sPHENIX electromagnetic calorimeter. This observable is sensitive to CT3 multiparton correlations in the proton.

2 sPHENIX detector

sPHENIX [8, 9] is a state-of-the-art detector designed to measure jet and heavy-flavor probes of the quark-gluon plasma (QGP) created in Au+Au collisions at the Relativistic Heavy-Ion Collider (RHIC) [10]. A precision tracking system enables measurements of heavy flavor and jet substructure observables, while the electromagnetic and hadronic calorimeter system is crucial for measuring the energy of jets and identifying direct photons and electrons.

Going outwards starting from the beam line, sPHENIX comprises the following subsystems [11]: the Vertex Detector (MVTX) based on Monolithic Active Pixel Sensors (MAPS) technology; the INTermediate Tracker (INTT); the Time Projection Chamber (TPC) [12]; the Time Projection Chamber Outer Tracker (TPOT) [13]; the Electromagnetic Calorimeter (EMCal) [14, 15]; the Inner Hadronic Calorimeter (IHCal) [15]; the 1.4 T superconducting solenoid magnet [16] and the Outer Hadronic Calorimeter (OHCal) [15]. Except for TPOT, all detectors have full azimuthal coverage and span $|\eta| < 1.1$ in pseudorapidity. sPHENIX also includes a number of forward detectors, namely the Minimum Bias Detectors (MBD), the sPHENIX Event Plane Detectors (sEPD), and the Zero Degree Calorimeters (ZDC), which include the Shower Maximum Detector (SMD).

During RHIC Run-2024, sPHENIX collected a large sample of p+p physics data alongside a smaller sample of Au+Au data to complete its commissioning phase in that collision system.

3 Data Selection and analysis

The EMCal calibration and clustering is handled centrally [17] and the analyzed data are required to pass quality checks for the EMCal, the MBD, and the measured RHIC proton polarization. A preliminary analysis of the proton spin direction at the sPHENIX interaction point using the ZDCs and SMDs confirmed that the polarization is vertical at sPHENIX. The photon trigger system utilizes localized energy sums from a non-overlapping 8×8 tower grid window corresponding to (pseudorapidity $\times$ azimuth) = $\Delta\eta \times \Delta\phi = 0.19 \times 0.19$. In order for an event to be included in this analysis, the photon trigger with energy threshold 3 GeV or 4 GeV is required to have fired. Then pairs of EMCal clusters are formed. These di-photon candidates are binned in transverse momentum p_T. In order to reduce the fraction of combinatorial background not originating from meson decays, the energy asymmetry between the two clusters is required to be no larger than 0.7. Lastly, in order to mitigate trigger bias, the energy of at least one of the clusters in a di-photon is required to be at or above the point at which the photon trigger is close to its full efficiency. Alternatively, the di-photon energy must fulfill the energy threshold requirement and the two clusters must be sufficiently close together in (η, ϕ)-space to have fired the same trigger window.

Since both RHIC beams were transversely polarized in Run-2024, the asymmetry extraction is performed on two independent data samples: once using the transverse polarization of the clockwise-going beam, while the polarization of the anti-clockwise beam is averaged over, and then vice versa. The presented asymmetry results are averaged over these two data sets after confirming their consistency.

Mesons are reconstructed by selecting di-photons based on their invariant mass. As demonstrated in Figure 1, windows of $\pm 3\sigma$ width around each of the meson peaks define the π^0- and η-meson signal regions. The di-photon count rates N in the π^0 (η) signal region are sorted according to their azimuthal angle ϕ relative to the proton spin orientation (up $\uparrow$ or down $\downarrow$). Then the raw asymmetry

$$\epsilon(\phi) = \frac{\sqrt{N^{\uparrow}(\phi)N^{\downarrow}(\phi+\pi)} - \sqrt{N^{\downarrow}(\phi)N^{\uparrow}(\phi+\pi)}}{\sqrt{N^{\uparrow}(\phi)N^{\downarrow}(\phi+\pi)} + \sqrt{N^{\downarrow}(\phi)N^{\uparrow}(\phi+\pi)}}, \quad \phi \in [0, \pi] \tag{1}$$

is extracted, which cancels acceptance effects to first order. The raw asymmetry amplitude ϵ is determined by fitting a sinusoid:

$$\epsilon(\phi) = -\epsilon \cdot \sin(\phi). \tag{2}$$

This procedure is performed for different bins in di-photon $p_T > 3$ GeV with bin widths of 1 GeV up to 8 GeV and then wider bins. The highest p_T bin for the π^0-meson analysis is $8 < p_T/\text{GeV} < 10$. There is one more bin for the η-meson analysis, $10 < p_T/\text{GeV} < 20$, which is possible because cluster merging starts at higher p_T for the heavier meson. Figure 2 shows the sinusoidal behavior in one example p_T bin for each meson mass window. In each di-photon p_T bin, ϵ is extracted as the $\sin(\phi)$-amplitude of the fit, while the fit uncertainty is used as its statistical uncertainty $\delta\epsilon$.

To take into account that the proton beams were not polarized at 100%, the raw asymmetry

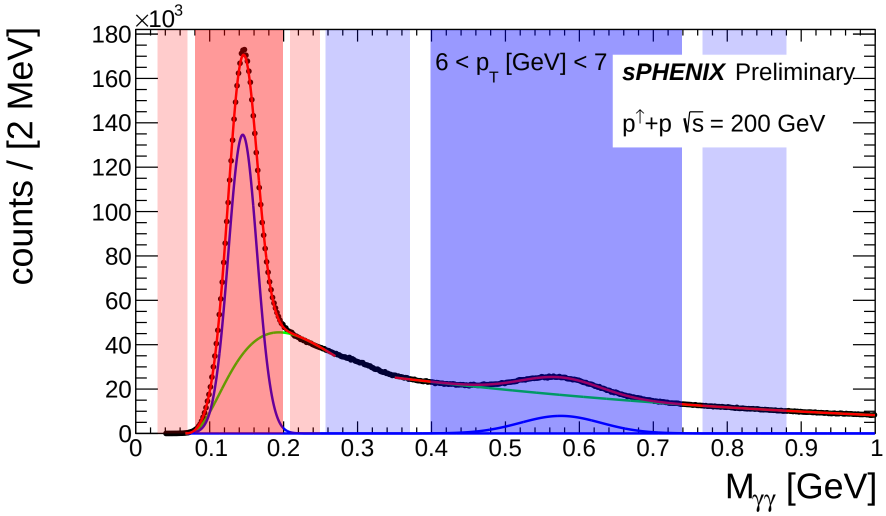

Figure 1: Invariant di-photon mass for an example p_T bin. The π^0 and η signal (background) regions are indicated by the dark (light) shaded areas. The data are fit with a Gaussian to determine the peak location (mean) and width (σ), superimposed on a threshold function with exponential to describe the background. The background fraction r is determined from fit integrals.

is scaled by the proton polarization P to obtain the asymmetry measured in the signal region $A_N^{\text{sig}} = 1/P \cdot \epsilon$. The proton polarization was about 50% in RHIC Run-2024. The asymmetry A_N^{sig} contains the mesons of interest, but also combinatorial background contributions. Since it is not possible to correct for background on an event-by-event basis with this type of traditional analysis, a background asymmetry A_N^{bg} is determined using di-photons with mass far away from the meson peaks, in the regions $\pm(3.5 - 5.5)\sigma$, as indicated by the light shaded areas in Figure 1. The physics asymmetry is then determined in each p_T bin as

$$A_N = \frac{A_N^{\text{sig}} - rA_N^{\text{bg}}}{1 - r}, \tag{3}$$

where r is the background fraction determined from the fit integrals in Figure 1 as the ratio of background / (meson + background) di-photon counts. The background fractions vary between approximately 35% and 50% for the π^0-meson with increasing trend to higher p_T bins, while they are around 85% for the η-meson and slightly higher in the last p_T bin. The meson selection procedure described here is in a preliminary stage. A future revised version of this analysis will incorporate additional information on the transverse shape of EMCal clusters, to more reliably reject clusters originating from sources other than single photons, thereby reducing combinatorial background and in turn these preliminary background fractions.

The statistical uncertainty δA_N of the physics asymmetry A_N is obtained by propagating the statistical uncertainties of the signal-region asymmetry A_N^{sig}, the background asymmetry A_N^{bg}, and the background fraction r in Equation 3 to δA_N. This procedure increases the statistical uncertainties because background contributions are removed. As with A_N itself, δA_N is scaled by $1/P$.

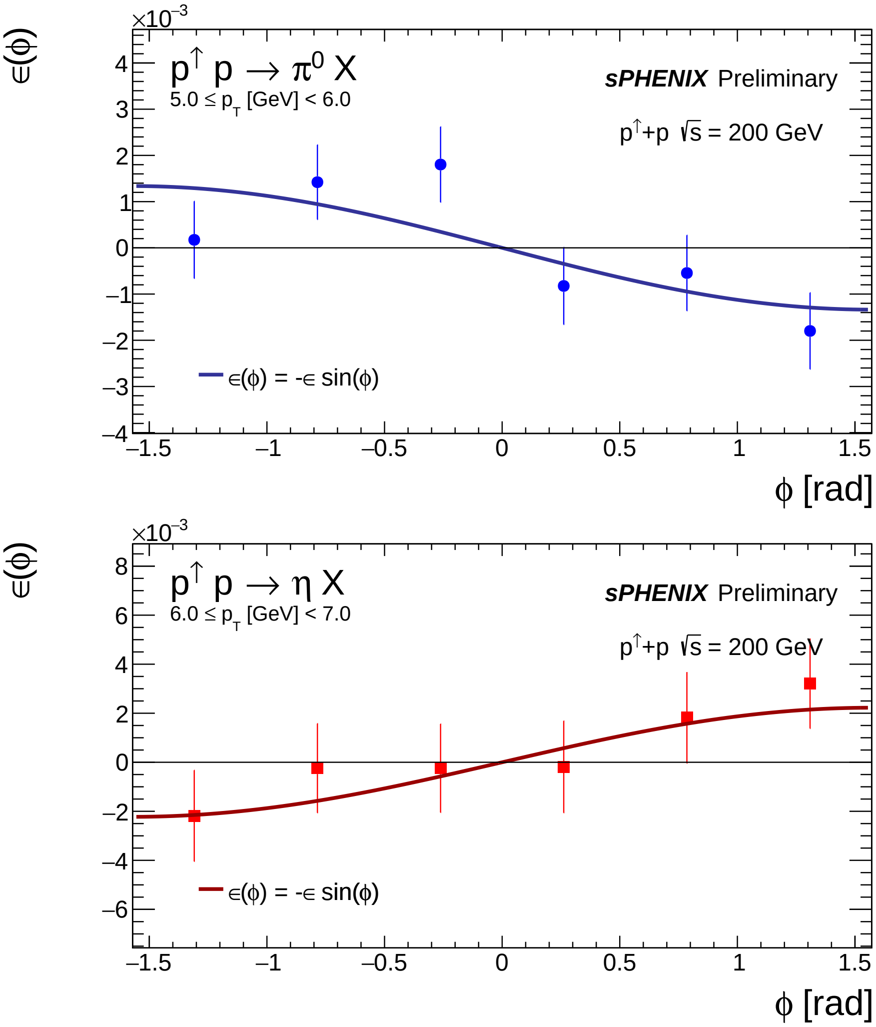

Figure 2: Raw asymmetry $\epsilon(\phi)$ extracted in example p_T bins for di-photons in the the π^0- (top) and η-meson (bottom) mass windows, when the anti-clockwise beam is taken as transversely polarized.

4 Systematic uncertainties

Three sources of systematic uncertainties are considered in this analysis.
1) **Extraction method:** the systematic uncertainty is taken as the difference between the primary "geometric mean" method of calculating A_N as in Equation 1 and an alternative method [18] that includes the relative luminosity between bunches of opposite transverse polarization directions, as measured by the MBD.
2) **Background fraction:** the uncertainty in subtracting the background is determined by using an alternative background fit function to extract an alternative background fraction. The systematic uncertainty is taken as the difference in A_N determined with the default background fit (see Figure 1) and that determined with the alternative fit.
3) **False asymmetries:** possible instrumental effects that could (unphysically) cause non-vanishing A_N are investigated by shuffling the physical polarization pattern of the 2×111 filled RHIC

bunches 10,000 times and checking for deviations in the pull distributions $A_N/\delta A_N^{\text{stat}}$ that are beyond the expected purely statistical fluctuations. While the means of the shuffled and Gaussian-fitted distributions are all found to be consistent with zero as expected, their widths σ_{fit} are found in some p_T bins to be larger than 1. In these bins, a systematic uncertainty $\delta A_N^{\text{sys,shuffle}}$ is assigned as

$$\delta A_N^{\text{sys,shuffle}} = A_N^{\text{stat}} \sqrt{\sigma_{\text{fit}}^2 - 1}. \tag{4}$$

There is no single dominating systematic uncertainty. Uncertainty 3) is assigned only in the four lower p_T bins for the π^0-meson, while it is present in all p_T bins for the η-meson and dominating there in the high p_T bins. The three sources of systematic uncertainty are combined quadratically. The systematic uncertainties are less than the statistical uncertainties in all p_T bins, and the latter dominate the former in most bins.

This analysis uses the online RHIC Run-2024polarization values, as the calibrated polarization values are not yet available. At this time, a 7% scale uncertainty [19] is assigned due to the measurement of the beam polarization, as noted in Figures 3 and 4. Such an uncertainty scales both central asymmetry values and their statistical uncertainties in the same way and therefore does not change the statistical significance relative to $A_N = 0$.

5 Results

Figure 3 shows the preliminary result of the p_T-binned A_N in inclusive π^0- and η-meson production together with its statistical and systematic uncertainties.

A comparison with the PHENIX Run-2015 measurement [18] is shown in Figure 4. The PHENIX measurement corresponds to $|\eta| < 0.35$ and that of sPHENIX to $\eta > 0$. Here, η is the pseudorapidity defined with respect to the polarized beam: $\eta > 0$ corresponds to the "forward" direction (x-Feynman $x_F > 0$) and $\eta < 0$ to the "backward" direction ($x_F < 0$). Figure 4 also indicates the sPHENIX average pseudorapidity values, $\langle\eta\rangle$, in each p_T bin. The new sPHENIX measurement is compatible with zero and consistent with the PHENIX data at $\langle\eta\rangle = 0$.

The integrated luminosity is about 35/pb for the sPHENIX measurement, while that of the PHENIX measurement is about 60/pb. The background fractions at sPHENIX are higher than at PHENIX. This causes the background correction at sPHENIX to increase the statistical uncertainties to a relatively larger extent. Secondly, the polarization for the sPHENIX data was around 50%, while that for the PHENIX data was around 59%. A combination of these two effects causes the statistical uncertainties of the two asymmetry measurements to not scale with their respective integrated luminosities. In a future revised version of this analysis, the sPHENIX meson selections are expected to be improved, while decreasing the background fractions.

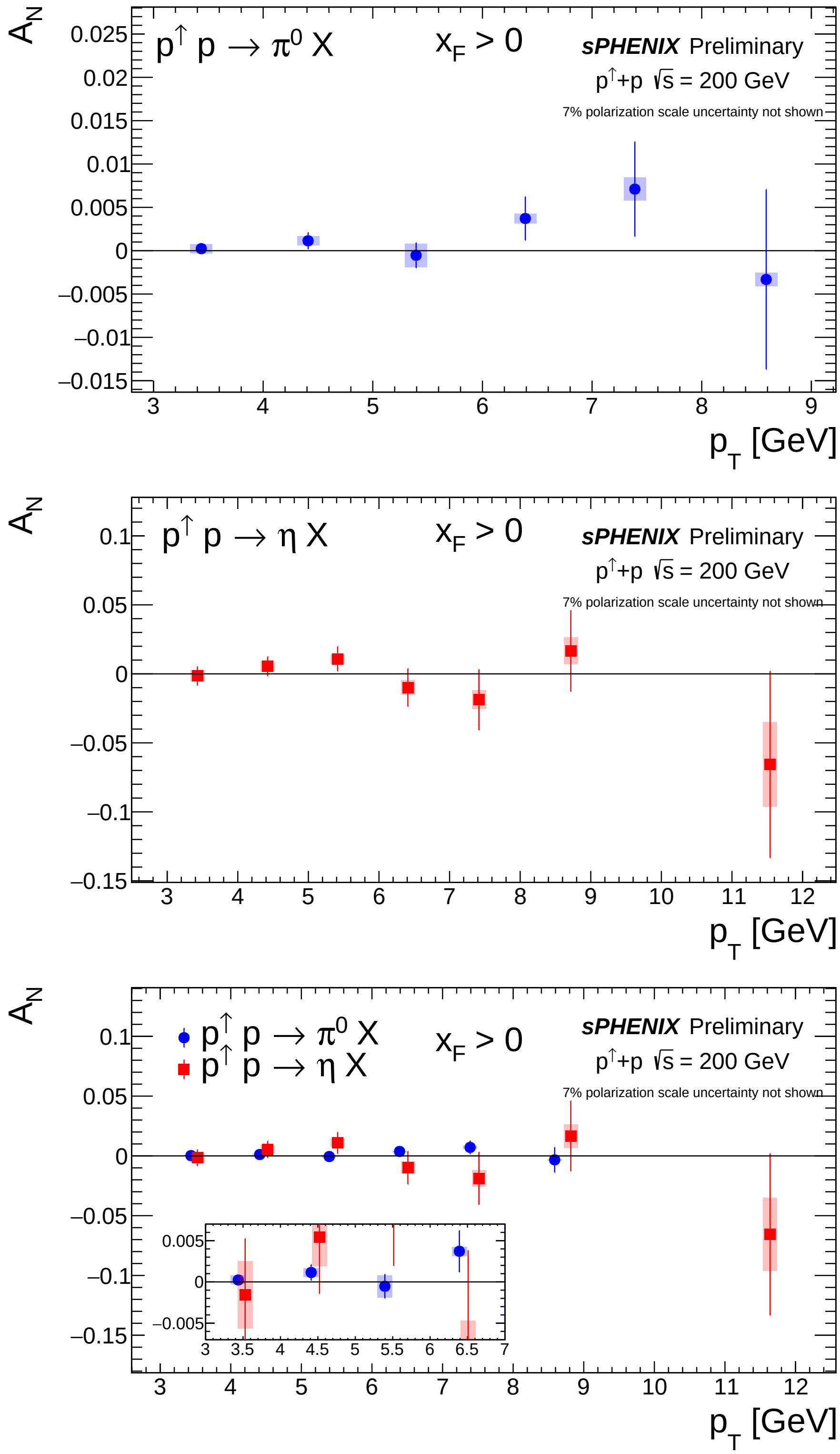

Figure 3: Preliminary sPHENIX results of the transverse single-spin asymmetry versus di-photon transverse momentum p_T in inclusive production of π^0-mesons (top) and η-mesons (middle), and a comparison between π^0- and η-meson results (bottom), in collisions of transversely polarized protons at $\sqrt{s} = 200$ GeV. The error bars indicate the statistical uncertainties, the shaded boxes the systematic uncertainties. The η-meson points are slightly offset horizontally for better visibility.

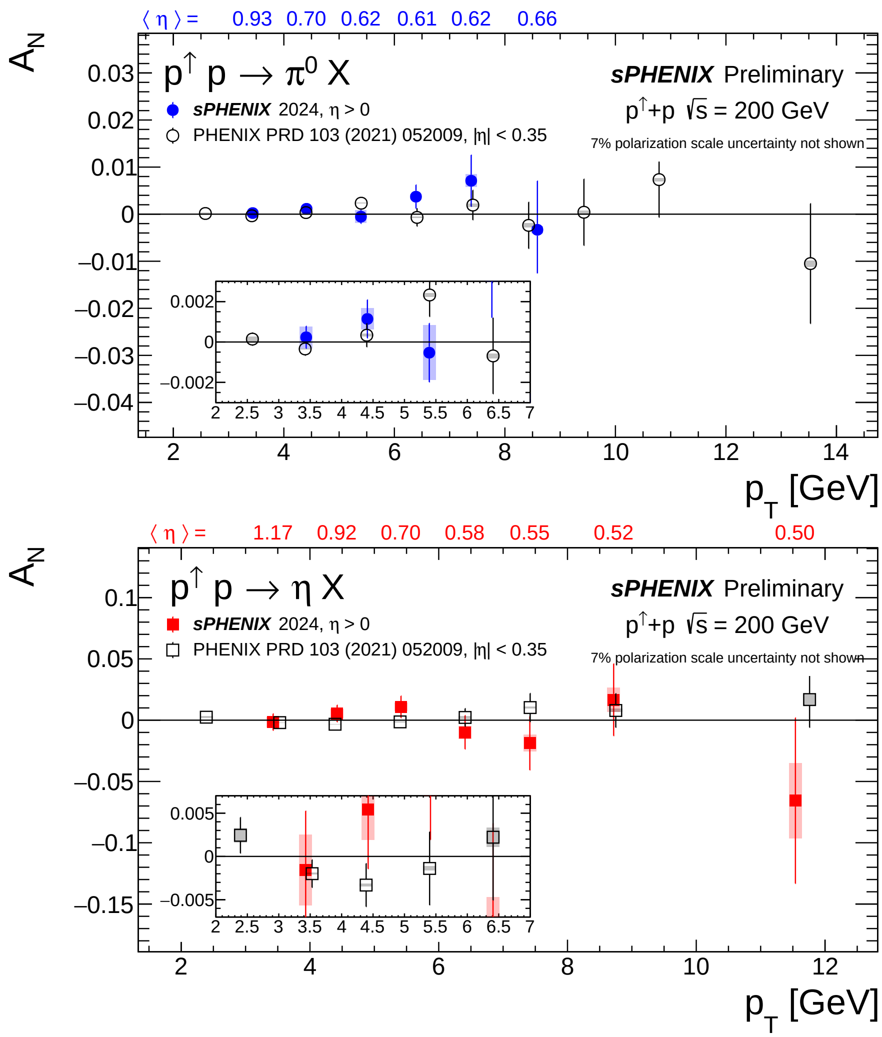

Figure 4: Preliminary sPHENIX Run-2024 results compared to PHENIX Run-2015 results [18] in inclusive production of π^0-mesons (top) and η-mesons (bottom) in collisions of transversely polarized protons at $\sqrt{s} = 200$ GeV. The error bars indicate the statistical uncertainties, the shaded boxes the systematic uncertainties. The average sPHENIX pseudorapidity values $\langle\eta\rangle$ are indicated for each p_T bin.

6 Conclusion

The first extraction of a transverse single-spin asymmetry A_N using the sPHENIX detector and the RHIC Run-2024 $\sqrt{s} = 200$ GeV $p^{\uparrow}+p$ data is presented. The analyzed channel is neutral light meson production in the di-photon decay channel, with the signatures of the decay photons registered in the sPHENIX electromagnetic calorimeter. The A_N is presented in bins of p_T for the π^0 and η mesons and a comparison to the PHENIX Run-2015 results is shown. A future revised version of this extraction will extend the analysis down to di-photon-$p_T > 1$ GeV. The new sPHENIX measurement at moderate forward rapidity is found to be compatible with zero and consistent with PHENIX data at midrapidity.

References

[1] Christine A. Aidala, Steven D. Bass, Delia Hasch, and Gerhard K. Mallot. The spin structure of the nucleon. *Rev. Mod. Phys.*, 85:655–691, Apr 2013. URL: https://link.aps.org/doi/10.1103/RevModPhys.85.655, doi:10.1103/RevModPhys.85.655. 1

[2] Dennis Sivers. Single-spin production asymmetries from the hard scattering of pointlike constituents. *Phys. Rev. D*, 41:83–90, Jan 1990. URL: https://link.aps.org/doi/10.1103/PhysRevD.41.83, doi:10.1103/PhysRevD.41.83. 1

[3] Dennis Sivers. Hard-scattering scaling laws for single-spin production asymmetries. *Phys. Rev. D*, 43:261–263, Jan 1991. URL: https://link.aps.org/doi/10.1103/PhysRevD.43.261, doi:10.1103/PhysRevD.43.261. 1

[4] John Collins. Fragmentation of transversely polarized quarks probed in transverse momentum distributions. *Nuclear Physics B*, 396(1):161–182, 1993. URL: https://www.sciencedirect.com/science/article/pii/055032139390262N, doi:10.1016/0550-3213(93)90262-N. 1

[5] Daniel Pitonyak. Transverse spin observables in hard-scattering hadronic processes within collinear factorization. *International Journal of Modern Physics A*, 31(32):1630049, 2016. doi:10.1142/S0217751X16300490. 1

[6] J. Cammarota, L. Gamberg, Z. Kang, Joshua A. Miller, Daniel Pitonyak, Alexei Prokudin, Ted C. Rogers, and Nobuo Sato. Origin of single transverse-spin asymmetries in high-energy collisions. *Phys. Rev. D*, 102:054002, Sep 2020. URL: https://link.aps.org/doi/10.1103/PhysRevD.102.054002, doi:10.1103/PhysRevD.102.054002. 1

[7] Xiangdong Ji, Jian-Wei Qiu, Werner Vogelsang, and Feng Yuan. Unified picture for single transverse-spin asymmetries in hard-scattering processes. *Phys. Rev. Lett.*, 97:082002, Aug 2006. URL: https://link.aps.org/doi/10.1103/PhysRevLett.97.082002, doi:10.1103/PhysRevLett.97.082002. 1

[8] A. Adare et al. An Upgrade Proposal from the PHENIX Collaboration. 2015. arXiv:1501.06197. 2

[9] Ron Belmont et al. Predictions for the sPHENIX physics program. *Nucl. Phys. A*, 1043:122821, 2024. doi:10.1016/j.nuclphysa.2024.122821. 2

[10] M. Harrison, T. Ludlam, and S. Ozaki. RHIC project overview. *Nucl. Instrum. Meth. A*, 499(2):235–244, 2003. doi:10.1016/S0168-9002(02)01937-X. 2

[11] The sPHENIX Collaboration. sPHENIX Technical Design Report, PD-2/3 Release, 2019. URL: https://indico.bnl.gov/event/7081/attachments/25527/38284/sphenix_tdr_20190513.pdf. 2

[12] Henry Klest. Overview and design of the sPHENIX TPC. *J. Phys. Conf. Ser.*, 1498:012025, 2020. arXiv:2110.02082, doi:10.1088/1742-6596/1498/1/012025. 2

[13] S. Aune et al. The sPHENIX Micromegas Outer Tracker. *Nucl. Instrum. Meth. A*, 1066:169615, 2024. doi:10.1016/j.nima.2024.169615. 2

[14] C. A. Aidala et al. Design and Beam Test Results for the 2-D Projective sPHENIX Electromagnetic Calorimeter Prototype. *IEEE Trans. Nucl. Sci.*, 68(2):173–181, 2021. doi:10.1109/TNS.2020.3034643. 2

[15] C. A. Aidala et al. Design and Beam Test Results for the sPHENIX Electromagnetic and Hadronic Calorimeter Prototypes. *IEEE Trans. Nucl. Sci.*, 65(12):2901–2919, 2018. doi:10.1109/TNS.2018.2879047. 2

[16] T. G. O'Connor et al. Design and testing of the 1.5 T superconducting solenoid for the BaBar detector at PEP-II in SLAC. *IEEE Trans. Appl. Supercond.*, 9:847–851, 1999. doi:10.1109/77.783429. 2

[17] The sPHENIX Collaboration. Measurement of π^0 v_2 in Au+Au Collisions at 200 GeV with the sPHENIX Detector, 2019. URL: https://www.sphenix.bnl.gov/sPH-CONF-BULK-2024-01. 3

[18] PHENIX Collaboration (U.A. Acharya et al.). Transverse single-spin asymmetries of midrapidity π^0 and η mesons in polarized $p+p$ collisions at $\sqrt{s} = 200$ GeV. *Phys. Rev. D*, 103(5):052009, 2021. arXiv:2011.14170, doi:10.1103/PhysRevD.103.052009. 4, 5, 4

[19] RHIC polarimetry group. Private communication, March 2025. 4